Stochastic resonance in periodic potentials

S. Saikia,[1,2] A. M. Jayannavar,[3] and Mangal C. Mahato[1,*]
[1]*Department of Physics, North-Eastern Hill University, Shillong-793022, India*
[2]*St. Anthony's College, Shillong-793003, India*
[3]*Institute of Physics, Sachivalaya Marg, Bhubaneswar-751005, India*
(Received 17 November 2010; revised manuscript received 15 March 2011; published 16 June 2011)

The phenomenon of stochastic resonance (SR) is known to occur mostly in bistable systems. However, the question of the occurrence of SR in periodic potential systems has not been resolved conclusively. Our present numerical work shows that the periodic potential system indeed exhibits SR in the high-frequency regime, where the linear-response theory yields maximum frequency-dependent mobility as a function of noise strength. The existence of two (and only two) distinct dynamical states of trajectories in this moderately feebly damped periodically driven noisy periodic potential system plays an important role in the occurrence of SR.

DOI: 10.1103/PhysRevE.83.061121 PACS number(s): 05.40.Jc, 05.60.Cd, 05.40.Ca

I. INTRODUCTION

Stochastic resonance (SR) was discovered theoretically about three decades ago [1]. Since then, SR has been investigated with vigor, and many notable reviews have appeared; see, for instance, [2,3]. Physical systems are always subject to internal or external (thermal or otherwise) fluctuations (noise). The optimal periodic response of a system to an external periodic drive as a function of noise strength is referred to as stochastic resonance. It has been experimentally found to occur in electronic circuits [4–6], two-mode ring lasers [7], nanomechanical systems [8], and neuronal systems [9–12], just to name a few. Its main attraction lies in its practical utility of selecting and enhancing a signal of a particular frequency out of a host of signals by tuning the noise strength. Presumably, biological systems use SR to their advantage [13]. It has the potential to be utilized to control kinetically the pathways of a biochemical reaction [14].

SR has been predicted and shown to occur mostly in bistable systems [2,15]. However, there have been some notable investigations of SR in monostable and also periodic potential systems [16,17]. In the monostable systems, SR is shown to occur in the high-frequency regime close to the natural frequency of oscillation at the bottom of the potential. However, the occurrence of SR in periodic potentials has not been conclusive [18].

Dykman and co-workers [17] used an interesting model in which a single-well Duffing oscillator with additive noise is driven at a frequency close to the natural frequency of the oscillator. The model is used under a linear-response theory formalism to study fluctuation phenomena associated with two coexisting periodic attractors. A weak Gaussian noise causes a transition between these two attractors. The populations of these two attractors become equal at a particular noise strength where the response becomes maximum. This is considered to be a genuine signature of a (nonconventional) stochastic resonance. The theoretical result was supported by an analog electronic circuit experiment. A similar result was obtained in an underdamped superconducting quantum interference device [19].

The same resonance behavior as in Ref. [17] in the frequency-dependent mobility was obtained by Kim and Sung [18] in a periodic potential using linear-response theory in the high-frequency range of the external periodic drive. However, these authors ascribe this resonant behavior as simply a noise-assisted standard dynamical resonance as the transitions involve only intrawell motion. Also, in the interwell hopping (low) frequency regime, the frequency-dependent mobility shows monotonic behavior as a function of noise strength, thereby discounting the possibility of the occurrence of SR in periodic structures. However, the authors show that SR can occur if the driven system has a tilted periodic potential so that the passages are allowed only in one direction.

Moreover, it was observed recently that in a bistable potential, $V(x) = V_0 e^{-ax^2} + b|x|^q/q$, the confinement parameter q plays an important role in deciding whether the system will show SR [20]. For $q \geqslant 2$ the system shows SR, whereas for $q < 2$ it does not. In addition, we find that the input energy expended per period of the external field on the system by the field acts as a good quantifier of SR [21]. This input energy is ultimately dissipated into the thermal bath. This is naturally a measure of the hysteresis loop area in position(x)-force(F) space. Although the input energy and hysteresis loop area are exactly the same in magnitude, the latter is an average quantity, whereas input energy has a well-defined distribution. The input energy distribution provides useful information about stochastic resonance behavior. In particular, the distribution shows a characteristic largest shoulder (bimodality) at stochastic resonance [22–24]. On the other hand, hysteresis loops carry important information about the phase relationship between x and F, which have also been of interest to SR [21,25,26].

In the present work, we explore the possibility of the occurrence of SR in a periodic sinusoidal potential using input energy and hysteresis loop area as quantifiers. Moreover, one can take various values of the wave vector k of the potential analogously varying the effect of the confinement parameter q of the bistable potential discussed above. However, we only present results for $k = 1$.

We find that the periodic sinusoidal potential does not show SR when driven by a low-frequency field corresponding to

*mangal@nehu.ac.in

Kramers rates across the maxima of the potential or when driven at a still lower frequency. The same conclusion was arrived at in Ref. [27] while studying the diffusion coefficient in a periodic system. However, it should be noted that in Ref. [27], the probability $P(\tau')$ of a particle, after going from one well to an adjacent one and returning back to the same initial well in the subsequent time τ', shows periodic peaks. The strength of the first peak of $P(\tau')$ shows SR-like behavior. However, $P(\tau')$ has, by construction, the bearings of a bistable system and not that of a periodic potential system.

We further find that in the high-frequency range, the input energy behaves similarly to the response function in the work of Dykman and co-workers [17] and to the frequency-dependent mobility in the work of Kim and Sung [18]. In addition, our work shows that the input energy peaks as a function of noise strength. This is an indication of SR arising due to a competition between two dynamical states of particle trajectories (to be elaborated in Sec. III) as in the case of bistable systems. Though the trajectories are intrawell in nature, close to SR the transition between these two states is also aided by interwell passages of particles across the potential maxima.

The two dynamical states of trajectories are distinctly identified by the phase difference ϕ between the periodic forcing $F = F_0\cos(\omega t)$ and the trajectory $x(t) = x_0\cos(\omega t + \phi)$, one having a fixed phase lag $\phi = \phi_1$ and the other $\phi = \phi_2$. Note that because the system at finite T is stochastic in nature, ϕ_1 and ϕ_2 are average quantities. These individual phase lags ϕ_1 and ϕ_2 effectively do not vary with the noise strength. However, the relative cumulative length of these two dynamical states in a trajectory changes with the noise strength. The average phase lag, therefore, changes with noise strength, similar to what was predicted and observed in Refs. [25,26] in the case of bistable systems. Moreover, the distribution of input energy shows very similar behavior across the input energy peak to that in the case of SR in a bistable system, thus affirming the genuineness of SR in the present periodic potential system.

We consider two model systems for our study. In one case, the medium is considered to have uniform friction, whereas in the other case, the friction is considered to be nonuniform. The nonuniform friction $\gamma(x)$ has an exact analogy in the resistively and capacitively shunted junction (RCSJ) model of the Josephson junction. In the RCSJ model, the "$\cos\phi$" term, arising out of the interference between the quasiparticle tunneling and the Cooper pair tunneling across the junction, is equivalent to the nonuniform part of $\gamma(x)$ in the present case. The systems with nonuniform friction, however, are not very rare and are not without practical relevance [28]. Since the potential is symmetric and periodic, the homogeneous system does not show any average mobility. The nonuniform system, however, shows an average current when driven by a sinusoidal forcing in the underdamped system [29].

Interestingly, for the uniform system, $\phi_1 \simeq -0.013\pi$ and $\phi_2 \simeq -0.5\pi$, whereas in the nonuniform case, $\phi_1 \simeq -0.025\pi$ and $\phi_2 \simeq -0.85\pi$. In either case, the trajectories have distributions of these two phases depending on the noise strength. This is reflected in the form of the $(x - F)$ hysteresis loops, and hence in the average response amplitude and phase lag. In the homogeneous case, the behavior of the average phase lag conforms only approximately to the SR prediction of [21,26], and in the other case it follows closely the observations of [25] in bistable systems.

II. THE MODEL

In this work, we consider the underdamped motion of a particle in a periodic potential $V(x) = -V_0\sin(kx)$, which is symmetric in space [about $kx = (2n+1)\pi/2$, $n = 0, \pm 1, \pm 2, \ldots$]. The system is driven periodically by an external forcing $F(t) = F_0\cos(\omega t)$. We study two cases of the system: when the friction coefficient $\gamma(x)$ is uniform ($=\gamma_0$) (system is homogeneous) and when the friction coefficient is space-dependent, $\gamma(x) = \gamma_0[1 - \lambda\sin(kx + \theta)]$ (system is inhomogeneous). In the latter case, the friction is periodic with the same periodicity as the potential, but it has a phase difference θ with it ($\theta \neq 0,\pi$). λ ($0 \leqslant \lambda < 1$) determines the degree of inhomogeneity of the system ($\lambda = 0$ corresponds to the homogeneous system).

A particle of mass m moving in a periodic potential $V(x) = -V_0\sin(kx)$ in a medium with friction coefficient $\gamma(x)$ and subjected to an external periodic forcing $F(t)$ is considered to be described by the Langevin equation

$$m\frac{d^2x}{dt^2} = -\gamma(x)\frac{dx}{dt} - \frac{\partial V(x)}{\partial x} + F(t) + \sqrt{\gamma(x)T}\,\xi(t), \quad (2.1)$$

$$m\frac{d^2x}{dt^2} = -\gamma_0\frac{dx}{dt} - \frac{\partial V(x)}{\partial x} + F(t) + \sqrt{\gamma_0 T}\,\xi(t). \quad (2.2)$$

Equation (2.1) is for the inhomogeneous system and Eq. (2.2) is for the homogeneous system. The temperature T is in units of the Boltzmann constant k_B. The inherent random fluctuations in the system are represented by $\xi(t)$, which satisfy the following statistics: $\langle\xi(t)\rangle = 0$ and $\langle\xi(t)\xi(t')\rangle = 2\delta(t - t')$. The equations are written in dimensionless units by setting $m = 1$, $V_0 = 1$, and $k = 1$. The Langevin equations, with reduced variables denoted again now by the same symbols corresponding to Eqs. (2.1) and (2.2), are written as

$$\frac{d^2x}{dt^2} = -\gamma(x)\frac{dx}{dt} + \cos x + F(t) + \sqrt{\gamma(x)T}\,\xi(t), \quad (2.3)$$

$$\frac{d^2x}{dt^2} = -\gamma_0\frac{dx}{dt} + \cos x + F(t) + \sqrt{\gamma_0 T}\,\xi(t). \quad (2.4)$$

The potential barrier between any two consecutive wells of $V(x)$ disappears at the critical field value $F_0 = F_c = 1$. The noise variable in the same symbol ξ satisfies similar statistics to those mentioned earlier.

III. NUMERICAL RESULTS

The trajectories $x(t)$ are obtained numerically [30] by solving the Langevin equations (2.3) and (2.4) corresponding to the inhomogeneous and the homogeneous system, respectively, with the amplitude of the drive field, $F_0 = 0.2$ and $\omega = 2\pi/\tau$, with $\tau = 8$. The value of ω is close to the natural frequency of the potential. At high temperatures T, the average behavior of these trajectories is the same regardless of the initial conditions. However, at low temperatures, and especially in the limit of deterministic motion, and at such a low field amplitude as $F_0 = 0.2$, the trajectories are intrawell in nature.

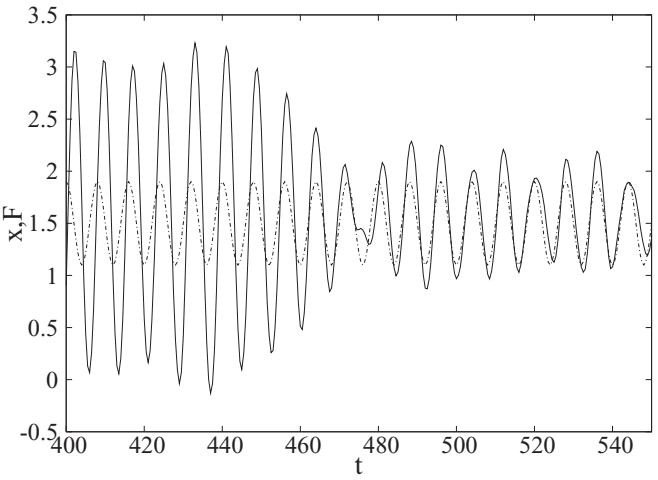

FIG. 1. Plot of $x(t)$ (solid line) and $F(t)$ (dot-dashed line) for $T = 0.015$. The particle exhibits both kinds of trajectories with a transition from out-of-phase to in-phase, in this case, at around $t = 460$; $\tau = 8$, $F_0 = 0.2$, and $\gamma_0 = 0.12$.

Yet their behavior is very sensitive to the initial conditions, $x(0) = x(t = 0)$ and $v(0) = v(t = 0)$ [31]. In our numerical calculations, we take $v(0) = 0$ and $x(0)$ at N equispaced intervals, x_i, $i = 1,2,\ldots,N$, between the two consecutive peaks, e.g., $[-\pi/2 < x_i \leqslant 3\pi/2]$, of the periodic potential $V(x)$. In most of the cases we take $N = 100$, but at some values of temperature we take $N = 300$.

Depending on the range of $x(0)$, we get two distinctly different kinds of trajectories, one that lags behind the applied field by a small phase difference ϕ_1 and the other by a large phase difference ϕ_2. For the sake of convenience, we call the former kind of trajectories *in-phase* and the other *out-of-phase*. The out-of-phase trajectories always have much higher amplitude than the in-phase trajectories; see Fig. 1. At the lowest temperature considered here, there is no transition between these dynamical states of trajectories. However, as the temperature (or the noise strength) is increased, transitions do take place (Fig. 1). Yet the trajectories are found basically only in these two states even at temperatures where interwell transitions lead the trajectories out of the initial well.

Following the stochastic energetics formulation of Sekimoto [32], the input energy, or work done by the field on the system W in a period τ, is calculated as

$$W(t_0,t_0+\tau) = \int_{t_0}^{t_0+\tau} \frac{\partial U(x(t),t)}{\partial t} dt, \tag{3.1}$$

where the potential $U(x(t),t) = V(x) - xF(t)$, $V(x) = -\sin(x)$, and $F(t) = F_0\cos(\omega t)$. The average input energy per period over an entire trajectory $\overline{W}$ is

$$\overline{W} = \frac{1}{N_1}\sum_{n=0}^{n=N_1} W(n\tau,(n+1)\tau). \tag{3.2}$$

Typically, the number of periods N_1 taken in a trajectory ranges between 10^5 and 10^7, as required. Finally, the average input energy per period $\langle\overline{W}\rangle$ is calculated by averaging $\overline{W}$ over all the trajectories. From Eq. (3.1), the distribution $P(W)$ is also calculated. As we shall see below, $P(W)$ provides an important complementary criterion for stochastic resonance.

Equation (3.1) can be further written as

$$W(t_0,t_0+\tau) = \int_{t_0}^{t_0+\tau} \frac{\partial U(x(t),t)}{\partial t} dt = -\int_{F(t_0)}^{F(t_0+\tau)} x\,dF, \tag{3.3}$$

which is the hysteresis loop area over a period. Since $x(t)$ is a stochastic variable, it is unreasonable to expect a sensible hysteresis loop over a period of the field. However, when averaged over the entire duration of a trajectory, a well-defined hysteresis loop $\overline{x}(F(t_i))$ and its area $\overline{A}$ are obtained:

$$\overline{x}(F(t_i)) = \frac{1}{N_1}\sum_{n=0}^{n=N_1} x(F(n\tau+t_i)) \tag{3.4}$$

for all $[0 \leqslant t_i < \tau]$, and

$$\overline{A} = |\overline{W}|. \tag{3.5}$$

The calculation of the hysteresis loops $\overline{x}(F(t_i))$, Eq. (3.3), is correct at the lowest temperatures where the trajectories maintain the same phase ϕ throughout, and also at higher temperatures where trajectories change phase between ϕ_1 and ϕ_2 during their journey. However, the hysteresis loops will be different for different trajectories depending on the cumulative duration of the dynamical states $\phi_{1,2}$ of the segments of the individual trajectories. Therefore, an ensemble average $\langle\overline{x}(F(t_i))\rangle$ is taken over all the trajectories considered. The hysteresis loop $\langle\overline{x}(F(t_i))\rangle$, with area $\langle\overline{A}\rangle$, reflects the average response $x(t)$ of the system to the applied field $F(t)$. In the linear-response regime, one would expect $x(t) = x_0\cos(\omega t + \overline{\phi})$ for $F(t) = F_0\cos(\omega t)$, $\omega = 2\pi/\tau$, where $\overline{\phi}$ is the average phase lag to be observed experimentally [25]. Notice that $\overline{\phi}$ will, in general, be different from the fixed phases ϕ_1 and ϕ_2 characterizing the individual dynamical phases of the trajectories.

In the following, we present the results of our numerical calculations and analyze how the particle trajectories in the sinusoidal potential, and hence the input energy and the hysteresis loops, are affected by noise strength. We examine the occurrence of stochastic resonance in the periodic potential, referring to the standard SR criteria in bistable systems.

A. Homogeneous systems

1. The intra- and interwell transitions and input energy

Figure 2(a) shows the plot of input energy $\overline{W}$ averaged over a trajectory with initial position $x(0)$ at the lowest temperature $T = 0.001$ for the homogeneous system $[\gamma(x) = \gamma_0]$. $\overline{W}$ are confined to two narrow bands around 0.094 and 1.179 corresponding to $x(0)$ values that lie in contiguous regions in the range $[-\pi/2,3\pi/2]$ and no points in between. The input energies $\overline{W} = 0.094$ correspond to in-phase trajectories with phase lag $\phi_1 \simeq -0.013\pi$, and those with $\overline{W} = 1.179$ correspond to out-of-phase trajectories with phase lag $\phi_2 \simeq -0.5\pi$. The trajectories continue to be in the same state of phase lag throughout their journey. At this low temperature, the trajectories are quite stable. The inset of Fig. 2(a) shows the $(x$-$v)$ plane Poincaré (stroboscopic) plots revealing the two attractors corresponding to the two dynamical states

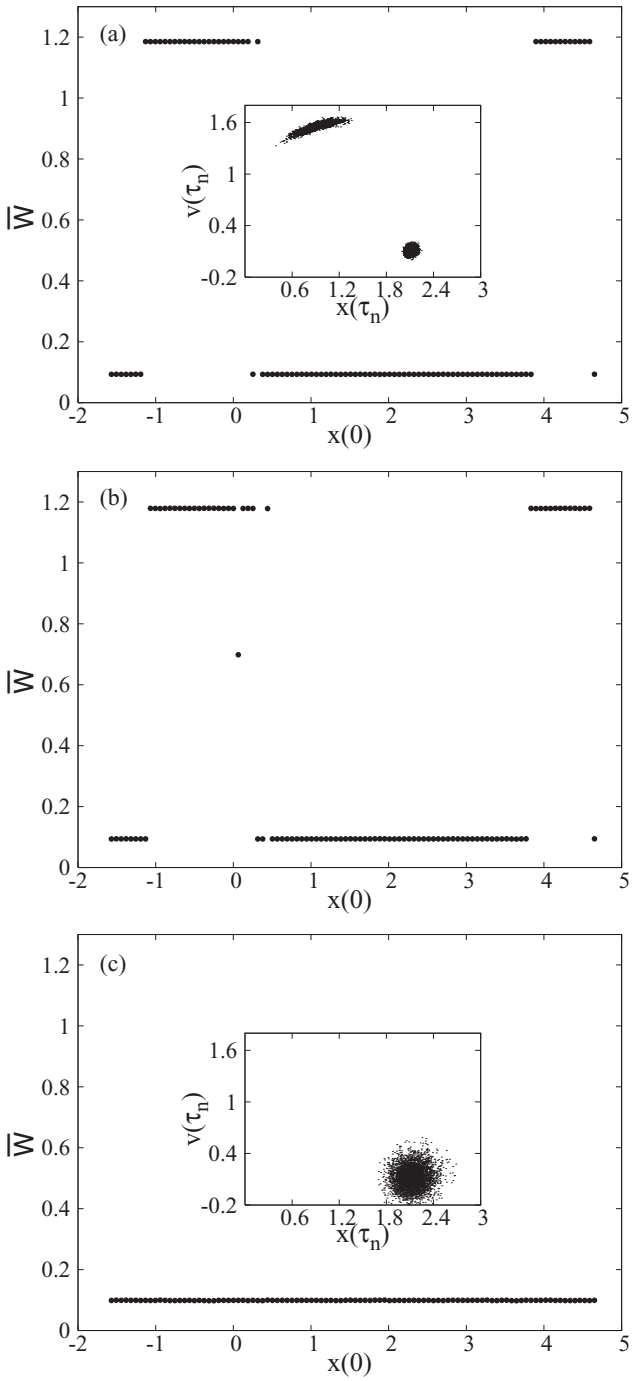

FIG. 2. Plot of $\overline{W}$ with $x(0)$ for $T = 0.001$ (a), $T = 0.003$ (b), and $T = 0.016$ (c); $\tau = 8$, $F_0 = 0.2$, and $\gamma_0 = 0.12$. The insets in (a) and (c) show the stroboscopic (Poincaré) plots in the $(x$-$v)$ plane at times $\tau_n = n\tau, n = 0, \pm 1, \pm 2, \cdots$

of the trajectories. The (stochastic) spread in the plots is due to the finite temperature of the system.

It may be recalled that the results are obtained by taking $v(0) = 0$. However, the two dynamical states of the trajectory are genuinely stable as revealed, in Fig. 3, by the basins of attraction of the two attractors at $T = 0.001$. In the figure, the in-phase and the out-of-phase states are indicated, respectively, by inp(l) and outp(m) for $l,m = 0, \pm 1, \pm 2$, etc. The indices l,m (within the parentheses) specify the well number where the

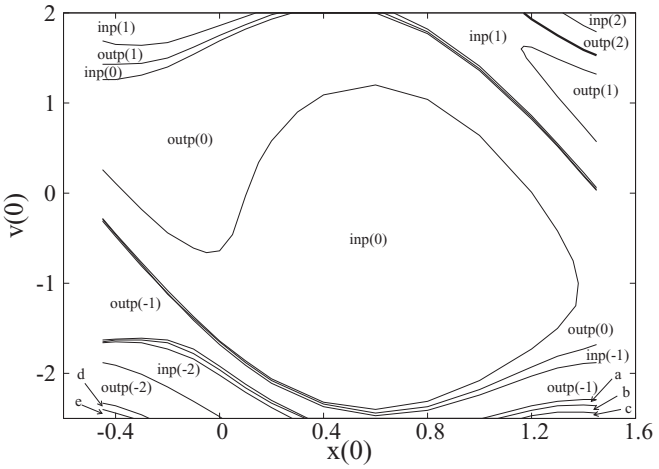

FIG. 3. The basins of attraction of the in-phase (inp) and out-of-phase (outp) attractors at temperature $T = 0.001$ are shown. The bracketed numbers on inp and outp indicate the well number of the periodic potential where the trajectory settles down in the in-phase or out-of-phase states. The region marked "a" corresponds to inp(-1), "b" corresponds to outp(-2), "c" corresponds to the continuation of inp(-2) indicated on the left side, "d" corresponds to inp(-3), and "e" corresponds to outp(-3). The boundaries correspond to the end of the phase indicated above the respective lines. The thick line separating outp(2) and inp(1) indicates that some other phases also chip in between. The phase inp(1) at the top right corner is just the continuation of the phase inp(1) on the left top corner of the figure. For this figure, $\tau = 8$, $F_0 = 0.2$, and $\gamma_0 = 0.12$.

particle settles down as it begins from the initial well $(l,m = 0)$. Even though the attractors correspond to wells $l,m \neq 0$, the phase and amplitude of the trajectories remain exactly the same as when they are in the initial well $(l,m = 0)$. Thus, the differently labeled trajectories are physically the same two and the only two: the in-phase and the out-of-phase with fixed ϕ_1 and ϕ_2, respectively.

Figure 2(b) shows the same plot as Fig. 2(a) but at $T = 0.003$. The figure clearly shows that a few points have deserted

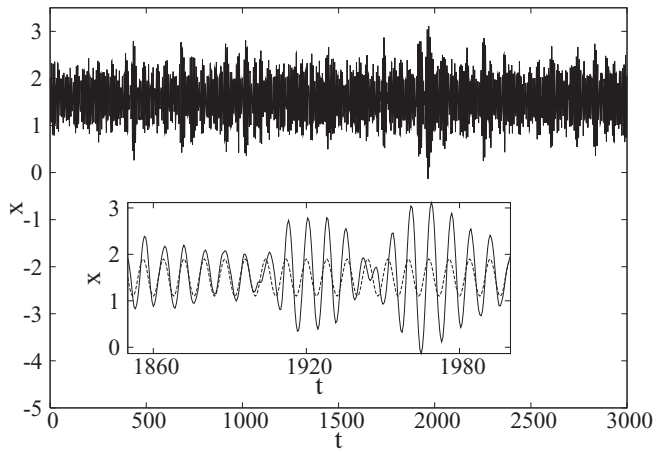

FIG. 4. Plot of the particle trajectories $x(t)$ for $T = 0.04$. Transitions are seen between the in-phase to the out-of-phase states. Inset is a magnified figure. $F(t)$ (dashed line) is also included for comparison; $x(0) = 2.0$, $\tau = 8$, $F_0 = 0.2$, and $\gamma_0 = 0.12$.

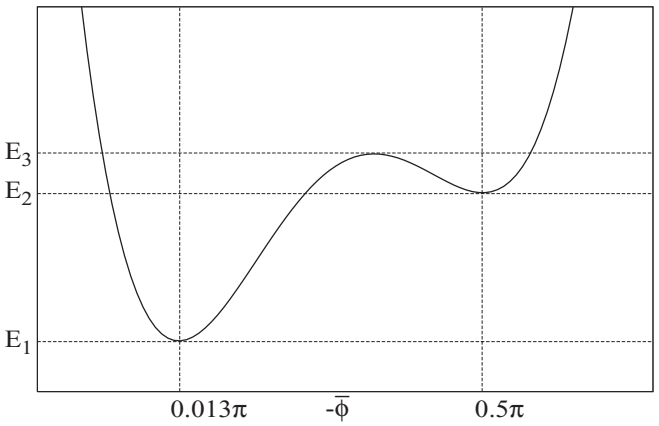

FIG. 5. A schematic depiction of the two dynamical energy states of the particle trajectories. In the figure, $E3 - E1 \simeq 0.016$ and $E3 - E2 \simeq 0.003$.

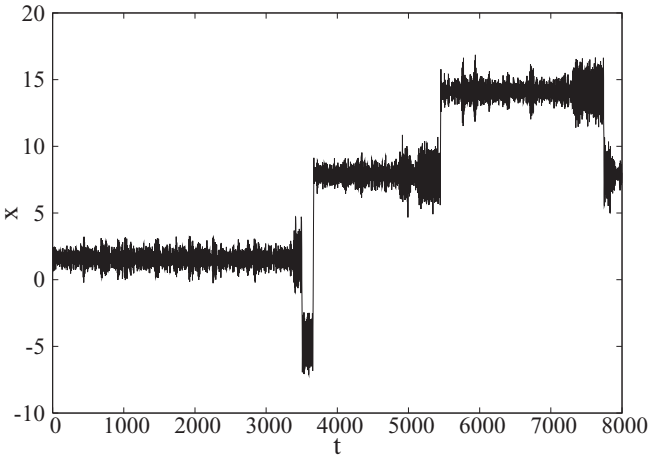

FIG. 6. Plot of $x(t)$ for $T = 0.08$. The figure shows interwell transitions as also numerous transitions between the in-phase (lower amplitude) and out-of-phase (higher amplitude) states. At around $t = 3700$ and 5400, the interwell jump also leads to a transition from the out-of-phase to the in-phase state; $x(0) = 2.0$, $\tau = 8$, $F_0 = 0.2$, and $\gamma_0 = 0.12$.

the upper band of $\overline{W}$, and all but one have already joined, with the lone one on its way to join the lower band of $\overline{W}$. This shows that all of these few out-of-phase trajectories have made a transition to the in-phase state (as shown in Fig. 1) quite early during the 10^5 periods of the trajectory, and the lone one has done so somewhere in the middle of all these periods. It should be noted that no transition has taken place from the in-phase state to the out-of-phase state. This shows that the out-of-phase state is less stable than the in-phase state, and they are separated by an energy barrier of about 0.003 (in units of V_0, the amplitude of the sinusoidal potential) from the out-of-phase side. This trend continues until $T = 0.016$, where $\overline{W}$ consists of only one band, i.e., the lower band [see Fig. 2(c)]. The stroboscopic plot in the $(x\text{-}v)$ space, inset of Fig. 2(c), shows the lone attractor at $T = 0.016$. The other attractor has now ceased to exist. From $T = 0.003$–0.016, the ensemble-averaged input energy $\langle \overline{W} \rangle$ decreases very rapidly attaining the lowest value at $T = 0.016$.

For $T > 0.016$, transitions start taking place from the in-phase to the out-of-phase state too. Consequently, $\langle \overline{W} \rangle$ begins rising for $T > 0.016$. Of course, the out-of-phase state lives for a very short duration before a larger temperature is reached. This is demonstrated in Fig. 4 for $T = 0.04$. Therefore, there is an energy barrier of roughly about 0.016 from the in-phase state side to the out-of-phase side. One can thus roughly picturize the two states as shown in Fig. 5 with the bottom of the wells at $-\phi_1 = 0.013\pi$ and $-\phi_2 = 0.5\pi$.

As the temperature is increased further, the relative population of the out-of-phase state keeps increasing with an increase of temperature. The transitions in both directions maintain a constant ratio at any given temperature. Moreover, by the temperature $T \sim 0.08$, the interwell transitions have already set in and have become numerous. These interwell transitions also help intrawell transitions; see Fig. 6. At around $T = 0.2$, the relative populations of both states become almost equal and the input energy $\langle \overline{W} \rangle$ peaks. $T = 0.2$, thus, falls in the region of kinetic phase transition [33] between the two dynamical states.

Beyond $T = 0.2$, the intrawell transitions become more frequent and so do the interwell transitions. The transition points or the attempted transition points lead to lower amplitude motion. This results in gradual lowering of $\langle \overline{W} \rangle$

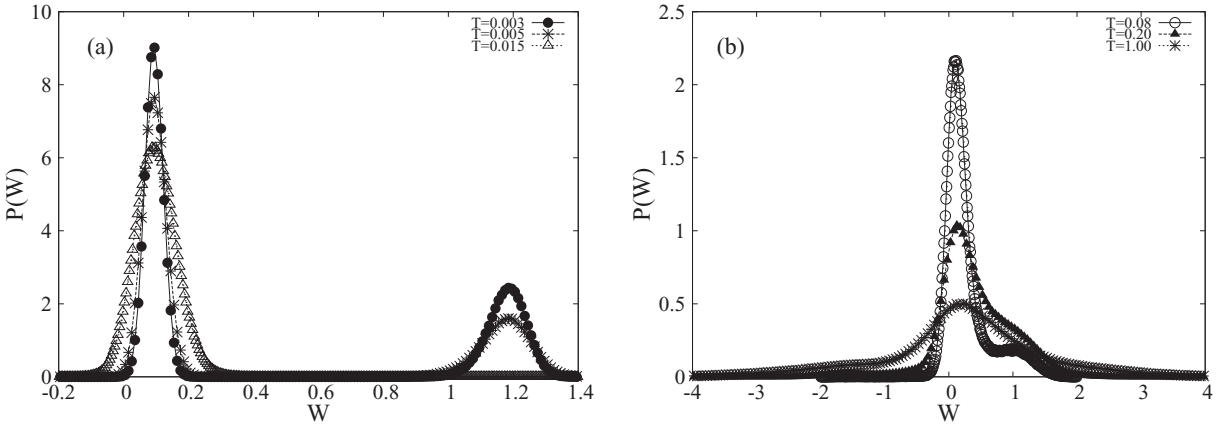

FIG. 7. Plot of $P(W)$ for different values of T [(a) for $T < 0.016$ and (b) for $T > 0.016$] for the homogeneous system. For large T, e.g., at $T = 1.0$, the distribution has a single peak structure; $\tau = 8$, $F_0 = 0.2$, and $\gamma_0 = 0.12$.

with temperature. At much higher temperatures $T \gg 0.2$, the (intrawell as well as interwell) transitions become so numerous that the phases effectively lose their distinct identity. This gets reflected in the input energy distribution $P(W)$ as a single peak (Fig. 7, $T = 1.0$).

In Fig. 7, the probability distribution of W is drawn for various temperatures. At the lowest temperature $T = 0.003$, we see two distinct peaks of $P(W)$: The low W peak corresponds predominantly to the in-phase state of the trajectory and the other to the out-of-phase state. As the temperature is gradually increased, the large W peak shrinks, and at $T = 0.016$ this peak disappears completely. However, as the temperature is increased further, the out-of-phase peak reappears and begins to swell to maximize at $T \sim 0.2$. At $T = 0.2$, the broad shoulder of $P(W)$ characterizes the peak in $\langle \overline{W} \rangle$. At the largest temperature shown, $T = 1.0$, both peaks merge into a broad single peak. It is interesting that, although $\langle \overline{W} \rangle$ always remains > 0, thus never violating the second law of thermodynamics, $P(W)$ is not confined to $W > 0$ but a significant part of it lies at $W < 0$.

Figure 8 shows the variation of $\langle \overline{W} \rangle$ as a function of temperature T. $\langle \overline{W} \rangle$ peaks at a temperature around $T = 0.2$. This is a clear signature of stochastic resonance even if the criterion for SR in a bistable system is adhered to as a benchmark [20,22,23]. This is supported by the behavior of $P(W)$ across $T = 0.2$. $P(W)$ shows a prominent shoulder [22,23], characteristic of SR, around $T = 0.2$ (Fig. 7). In the following, we examine the behavior of phase lag of the response to the periodic field.

2. *The hysteresis loop: Area and phase*

From Eqs. (3.3), (3.4), and (3.5), the hysteresis loop area $\langle \overline{A} \rangle$ being equal in magnitude to $\langle \overline{W} \rangle$, $\langle \overline{A} \rangle$ does not provide any additional information other than $\langle \overline{W} \rangle$. However, the hysteresis loop itself does give an important insight. The amplitude $F_0 = 0.2$ of the external applied field $F(t) = F_0 \cos(\omega t)$ being small, one expects the response, namely the position $x(t)$, to have a linear variation with $F(t)$: $x(t) = x_0 \cos(\omega t + \phi)$. Hence, the hysteresis loop $\langle \overline{x}(F(t_i)) \rangle$ will closely resemble an ellipse. The average phase difference $\overline{\phi}$ is measured from the resulting

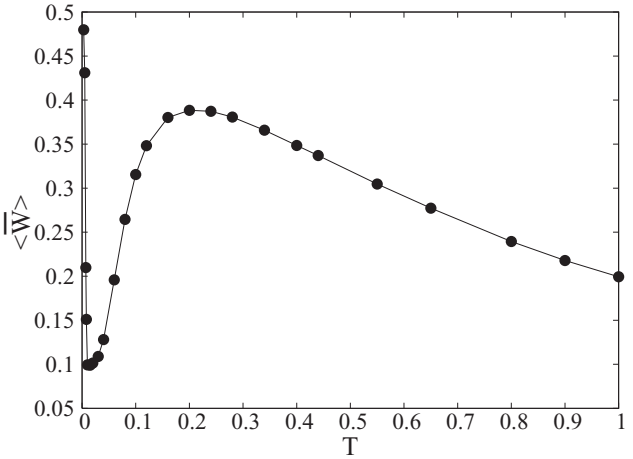

FIG. 8. Plot of $\langle \overline{W} \rangle$ as a function of T for the homogeneous system; $\tau = 8$, $F_0 = 0.2$, and $\gamma_0 = 0.12$.

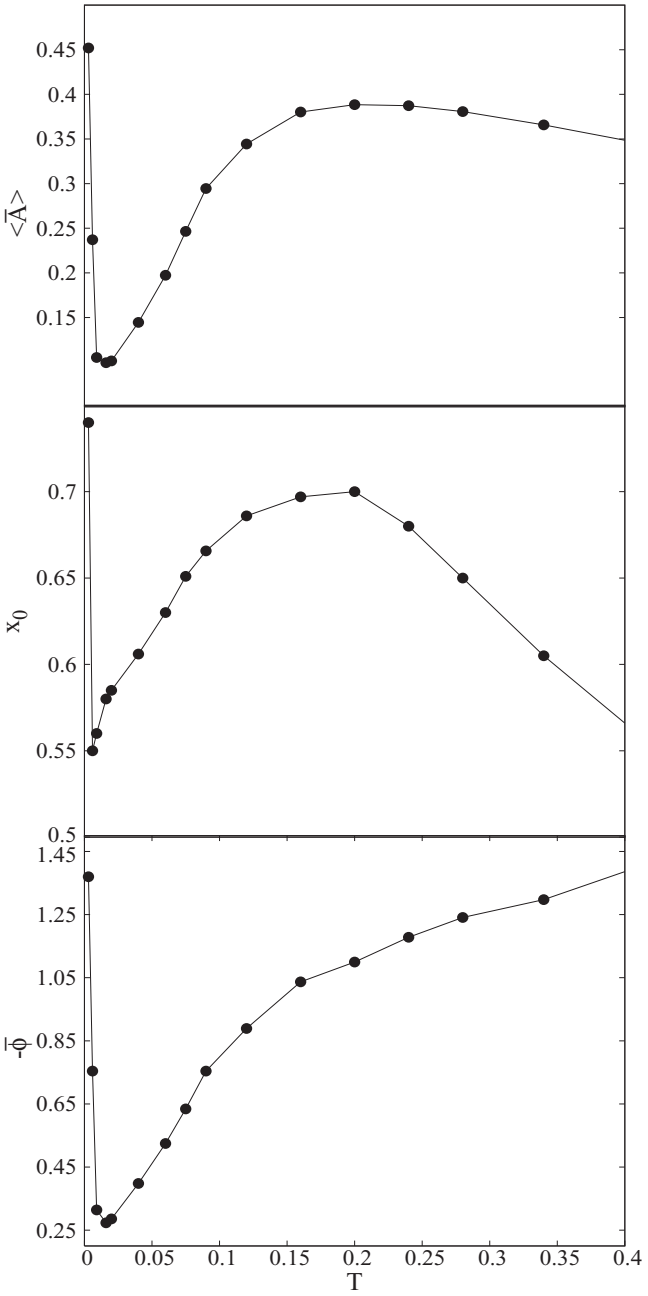

FIG. 9. Plot of $\langle \overline{A} \rangle$ (top), x_0 (middle), and $-\overline{\phi}$ (bottom) with T for the homogeneous system; $\tau = 8$, $F_0 = 0.2$, and $\gamma_0 = 0.12$. Beyond $T = 0.4$, the curves have a monotonic behavior and are not shown. The top figure is an exact reproduction of Fig. 8.

ellipse, Eq. (3.4). Unlike $\phi_1 \simeq -0.013\pi$ and $\phi_2 \simeq -0.5\pi$, which remain more or less constant with T, the average phase difference $\overline{\phi}$ varies with T, as shown in Fig. 9. In Fig. 9, the average amplitude x_0 and the average area $\langle \overline{A} \rangle$ are also plotted for comparison.

At the lowest temperature $T = 0.001$, $\overline{\phi}$ is close to $\phi_2 \simeq -0.5\pi$. At this temperature, x_0 as well as $\langle \overline{A} \rangle$ are also at their respective maxima. As T is increased, $-\overline{\phi}$ as well as $\langle \overline{A} \rangle$ decrease sharply, and attain a minimum at around $T = 0.016$. The minimum $\overline{\phi}$ is close to $\phi_1 \simeq -0.013\pi$. This is because at $T = 0.016$, all the trajectories are in the dynamical

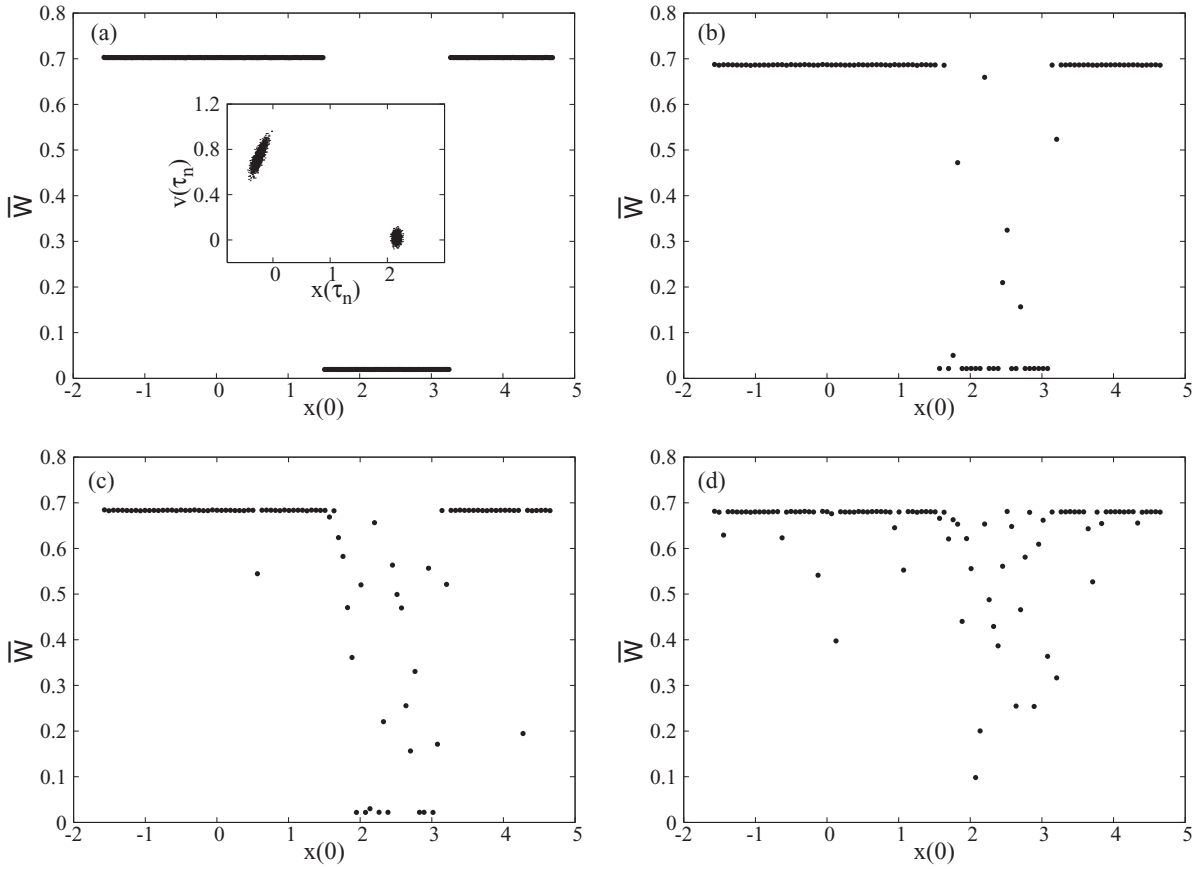

FIG. 10. Plot of $\overline{W}$ with $x(0)$ for $T = 0.001$ (a), $T = 0.012$ (b), $T = 0.014$ (c), and $T = 0.016$ (d); $\tau = 8$, $F_0 = 0.2$, and $\gamma_0 = 0.12$ for the inhomogeneous system. The inset of (a) shows the two attractors in the (x-v) plane stroboscopic plots at times $\tau_n = n\tau$.

state of phase ϕ_1. Thereafter for $T > 0.016$, $-\overline{\phi}$ increases monotonically. The inflection point of $-\overline{\phi}(T)$ occurs at $T \simeq 0.09$, where $-\overline{\phi} \simeq \pi/4$ as observed in Ref. [25]. However, $\langle \overline{A} \rangle$ becomes maximum only at a much higher temperature $T \simeq 0.2$, where $-\overline{\phi} \simeq 0.35\pi$. Therefore, $\langle \overline{A} \rangle$ here does not exactly satisfy the additional approximate SR criterion on $\overline{\phi}$ suggested in Ref. [25]. However, in the inhomogeneous system, the SR criterion on $\overline{\phi}$ suggested using linear-response theory [26] appears to be respected.

B. Inhomogeneous systems

In this case, the particle experiences nonuniform friction as it moves in the medium. As stated earlier, the potential is considered periodic: $V(x) = V_0 \sin(kx)$. The friction coefficient $\gamma(x)$ is taken as $\gamma(x) = \gamma_0[1 - \lambda \sin(kx + \theta)]$ instead of the constant friction coefficient $\gamma(x) = \gamma_0$ as in the homogeneous case. We take fixed values $\lambda = 0.9$ and phase difference $\theta = 0.35$ throughout. $\theta(\neq 0,\pi)$ provides the necessary asymmetry in the system to yield an average particle current, the ratchet current [31], even when driven by a zero time-average external forcing $F(t) = F_0 \cos(\omega t)$. For $k = 1$, $\gamma_0 = 0.12$, $F_0 = 0.7$, and $T = 0.4$, the system shows a current maximum at $\omega = 2\pi/140$. Keeping $\omega = 2\pi/\tau$, $\tau = 140$, and other parameters fixed, the current maximizes at $T \simeq 0.25$. However, we do not see any maximum in the periodic response, such as the hysteresis loop area, to the external periodic field corresponding to these parameters. The system does not show SR at this low frequency of drive.

Here, the particle position $x(t)$ roughly follows the periodic field with an irregular but large amplitude. There is also a small-amplitude high-frequency component superimposed on the low-frequency response to the field. The frequency of the superimposed component is close to the natural frequency of the potential. In the following, we consider the external field $F(t)$ with $F_0 = 0.2$ and $\tau = 8$, exactly as in the homogeneous case, but keeping in mind that in the inhomogeneous case the system is no longer symmetric. Therefore, even at this high frequency, the system shows an average ratchet current, but the current itself does not show any peaking behavior with T.

1. The intra- and interwell transitions and input energy

As in the homogeneous case, the system shows two distinct dynamical states of trajectories, one with phase difference $\phi_1 \simeq -0.025\pi$ and the other with $\phi_2 \simeq -0.85\pi$. We again refer to the trajectories with phase difference ϕ_1 as being in-phase and the other as out-of-phase with the external field, the latter having much higher response amplitude x_0 than the former. The frictional nonuniformity, surprisingly, leads to an out-of-phase trajectory amplitude about three times larger than in the homogeneous case, and therefore a larger average energy $\langle \overline{W} \rangle$. As a consequence, the results are qualitatively different from what was observed in the case of the uniform friction system.

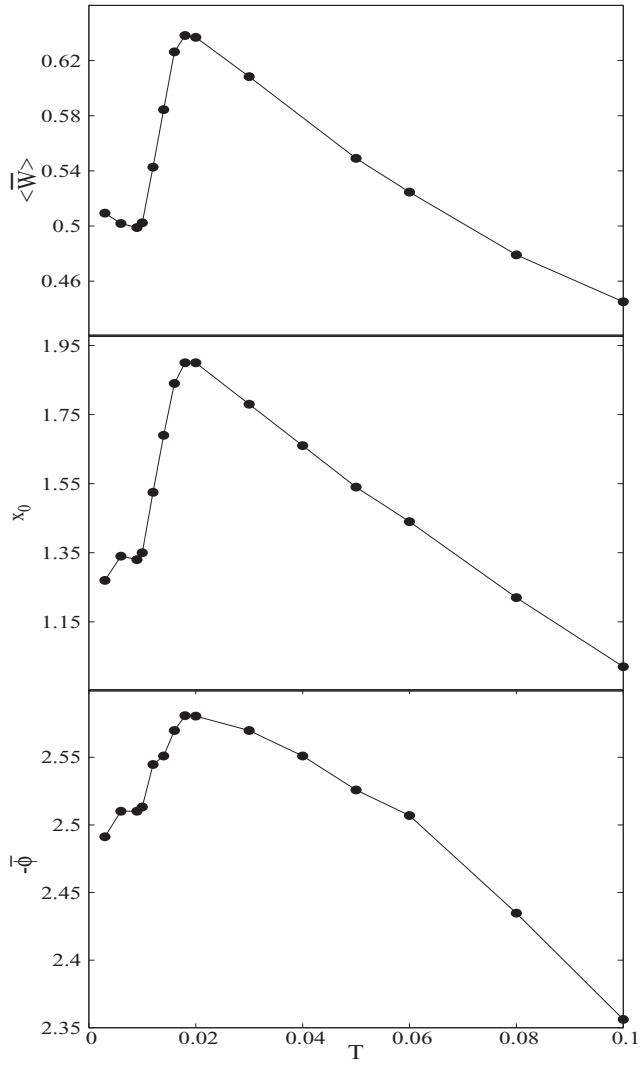

FIG. 11. Plot of $\langle \overline{W} \rangle$ (top), the amplitude x_0 (middle), and the phase difference $-\bar{\phi}$ (bottom) with T for the inhomogeneous system; $\tau = 8$, $F_0 = 0.2$, and $\gamma_0 = 0.12$.

At the lowest temperature $T = 0.001$, the trajectories are bunched into two contiguous groups and continue to be so for all time without ever jumping across the groups; see Fig. 10(a). The inset of Fig. 10(a) shows, in the $(x\text{-}v)$ plane stroboscopic plots, the two attractors corresponding to the two dynamical states of particle trajectories. The situation remains the same until $T = 0.01$. However, the average energy $\langle \overline{W} \rangle$ decreases with T due to a slight decrease in the out-of-phase trajectory amplitude. Contrast this with the sharp decline in energy in the homogeneous case due to the transition from out-of-phase states to in-phase states. At T around 0.011, transitions begin to take place from the in-phase states to the out-of-phase states [Fig. 10(b)]; the out-of-phase state is more stable. The $\langle \overline{W} \rangle$ rises sharply thereafter. However, by $T = 0.014$, transitions are also observed from out-of-phase states to in-phase states [Fig. 10(c)]. Therefore, the potential barrier from the out-of-phase side to the in-phase side is about 0.011, whereas in the reverse direction the barrier height is about 0.014. Both states are *almost* equally stable. By the temperature $T = 0.016$, even interwell transitions are observed [Fig. 10(d)].

As the temperature is increased to 0.018, the average energy $\langle \overline{W} \rangle$ attains a maximum. At this point, the two states become almost equally populated, a point in the region of the kinetic phase transition [33]. The variation of $\langle \overline{W} \rangle$ is plotted in Fig. 11 as a function of temperature. This is a signature of stochastic resonance occurring at $T = 0.018$. The distribution $P(W)$ again shows the largest asymmetry at the same temperature $T = 0.018$. Here $P(W)$ is distinctly bimodal in nature; see Fig. 12. For this nonuniform friction case, $P(W)$ behaves in a manner similar to the case of a homogeneous system (Fig. 7). However, unlike in the homogeneous case, here the out-of-phase state has the lowest energy. At $T = 0.018$, we have the largest contributing second peak of $P(W)$ to $\langle \overline{W} \rangle$ at any nonzero temperature. These intrawell transitions responsible for SR are effectively supported by numerous interwell transitions in the periodic potential system.

2. *The hysteresis loop: Area and phase*

Since the system is asymmetric and the amplitude x_0 is large, at low temperatures the hysteresis loops are not perfectly elliptical. Yet it is possible to roughly calculate the average amplitude x_0 and phase lags $-\bar{\phi}$ of the system response at all temperatures. In Fig. 11, x_0 and $-\bar{\phi}$ are also plotted along with $\langle \overline{W} \rangle$. It is clear from the figure that $\langle \overline{W} \rangle$, x_0, and $-\bar{\phi}$ all peak at almost the same temperature. Interestingly, the peak value of $-\bar{\phi}$ is about 0.82π. For this system, $-\bar{\phi}$ satisfies the peaking criterion of SR stated using the linear-response theory [26]. However, with respect to magnitude, the phase lag $-\bar{\phi}$ is off by about $\pi/2$.

IV. DISCUSSION AND CONCLUSION

A periodic potential system driven by a periodic applied field of small subthreshold amplitude at a high frequency, close to the natural frequency of the periodic potential well bottoms, shows stochastic resonance. Here the average input energy per period of the field is considered as the quantifier of SR. The same quantifier had served SR correctly in bistable systems. Moreover, the probability distribution of the input energy exhibits similar qualitative behavior at SR to that shown in the bistable systems. The linear-response theory calculated frequency-dependent mobility was found to show similar behavior to the input energy and was previously termed as merely a dynamical resonance. It was argued that the period of the drive was too small compared to the Kramers time of interwell static potential barrier crossing, thus disqualifying the resonance behavior from being a genuine stochastic resonance. However, we find that such an argument does not hold because, in the dynamical situation, the interwell transitions become quite numerous at the temperature where the input energy peaks. Moreover, and most importantly, the intrawell trajectories show bistability and the obtained resonance is a result of the transition between these dynamical states effectively helped by interwell transitions.

There have been two conflicting SR criteria involving the phase lag between the response and the applied field: one [25] stating that the phase lag shows inflection at SR with the phase lag equaling $\pi/4$, and the other [26] that phase lag shows a

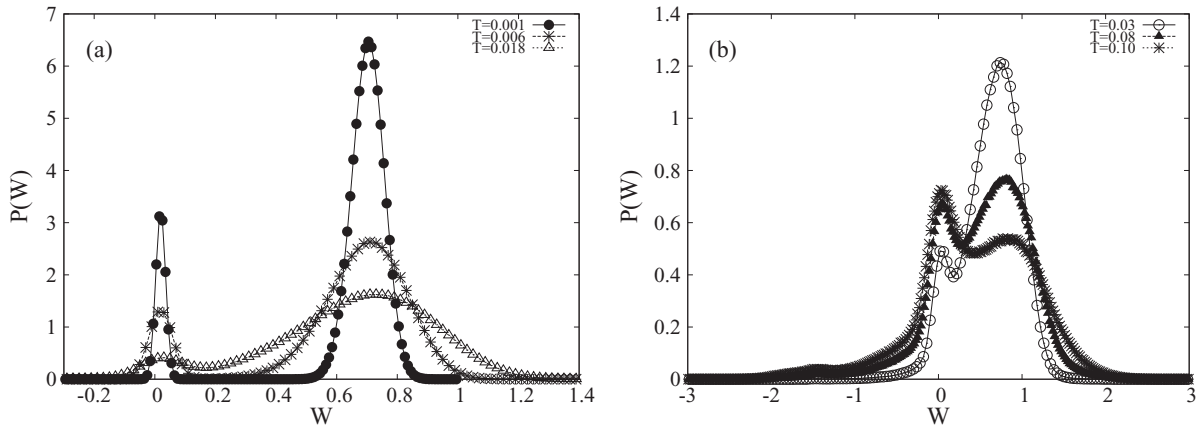

FIG. 12. Plot of $P(W)$ for different values of T [(a) for low T and (b) for higher T] for the inhomogeneous system; $\tau = 8$, $F_0 = 0.2$, and $\gamma_0 = 0.12$.

peak at SR. We find that whereas the former criterion is only approximately satisfied in the uniform friction case, the latter is satisfied for the nonuniform friction case. Thus, these criteria seem to be true for specific systems, and hence the phase lag $\overline{\phi}$ cannot be taken as a universal quantifier such as the input energy for SR.

ACKNOWLEDGMENTS

M.C.M. and A.M.J. acknowledge partial financial support from BRNS, DAE, India under Project No. 2009/37/17/BRNS/1959. A.M.J. thanks DST, Govt. of India for financial support.

[1] R. Benzi, A. Sutera, and A. Vulpiani, J. Phys. A **14**, L453 (1981).
[2] L. Gammaitoni, P. Hänggi, P. Jung, and F. Marchesoni, Rev. Mod. Phys. **70**, 223 (1998).
[3] T. Wellens, V. Shatokhin, and A. Buchleitner, Rep. Prog. Phys. **67**, 45 (2004).
[4] S. Fauve and F. Heslot, Phys. Lett. A **97**, 5 (1983).
[5] R. N. Mantegna and B. Spagnolo, Phys. Rev. E **49**, R1792 (1994).
[6] K. Murali, S. Sinha, W. L. Ditto, and A. R. Bulsara, Phys. Rev. Lett. **102**, 104101 (2009).
[7] B. McNamara, K. Wiesenfeld, and R. Roy, Phys. Rev. Lett. **60**, 2626 (1988).
[8] R. L. Badzey and P. Mohanty, Nature (London) **437**, 995 (2005).
[9] J. K. Douglass, L. Wilkens, E. Pantazelou, and F. Moss, Nature (London) **365**, 337 (1993).
[10] J. J. Collins, T. T. Imhoff, and P. Grigg, J. Neurophysiol. **76**, 642 (1996).
[11] B. J. Gluckman, T. I. Netoff, E. J. Neel, W. L. Ditto, M. L. Spano, and S. J. Schiff, Phys. Rev. Lett. **77**, 4098 (1996).
[12] E. Simonotto, M. Riani, C. Seife, M. Roberts, J. Twitty, and F. Moss, Phys. Rev. Lett. **78**, 1186 (1997).
[13] K. Wiesenfeld and F. Moss, Nature (London) **373**, 33 (1995).
[14] P. K. Ghosh, B. C. Bag, and D. S. Ray, Phys. Rev. E **75**, 032101 (2007).
[15] B. McNamara and K. Wiesenfeld, Phys. Rev. A **39**, 4854 (1989).
[16] N. G. Stocks, P. V. E. McClintock, and S. M. Soskin, Europhys. Lett. **21**, 395 (1993); N. G. Stocks, N. D. Stein, and P. V. E. McClintock, J. Phys. A **26**, L385 (1993).
[17] M. I. Dykman, D. G. Luchinsky, R. Mannella, P. V. E. McClintock, N. D. Stein, and N. G. Stocks, J. Stat. Phys. **70**, 479 (1993).
[18] Y. W. Kim and W. Sung, Phys. Rev. E **57**, R6237 (1998).
[19] I. Kh. Kaufman, D. G. Luchinsky, P. V. E. McClintock, S. M. Soskin, and N. D. Stein, Phys. Lett. A **220**, 219 (1996).
[20] E. Heinsalu, M. Patriarca, and F. Marchesoni, Eur. Phys. J. B **69**, 19 (2009).
[21] T. Iwai, Physica A **300**, 350 (2001).
[22] S. Saikia, R. Roy, and A. M. Jayannavar, Phys. Lett. A **369**, 367 (2007).
[23] M. Sahoo, S. Saikia, M. C. Mahato, and A. M. Jayannavar, Physica A **387**, 6284 (2008).
[24] P. Jop, A. Petrosyan, and S. Ciliberto, Europhys. Lett. **81**, 50005 (2008).
[25] L. Gammaitoni, F. Marchesoni, M. Martinelli, L. Pardi, and S. Santucci, Phys. Lett. A **158**, 449 (1991).
[26] M. I. Dykman, R. Mannella, P. V. E. McClintock, and N. G. Stocks, Phys. Rev. Lett. **68**, 2985 (1992); L. Gammaitoni and F. Marchesoni, *ibid.* **70**, 873 (1993); M. I. Dykman, R. Mannella, P. V. E. McClintock, and N. G. Stocks, *ibid.* **70**, 874 (1993).
[27] J. Kallunki, M. Dubé, and T. Ala Nissila, J. Phys. Condens. Matter **11**, 9841 (1999).
[28] W. L. Reenbohn and M. C. Mahato, J. Stat. Mech. (2009) P03011, and references therein.
[29] W. L. Reenbohn, S. Saikia, R. Roy, and M. C. Mahato, Pramana J. Phys. **71**, 297 (2008).
[30] R. Mannella, *A Gentle Introduction to the Integration of Stochastic Differential Equations*, in *Stochastic Processes in Physics, Chemistry, and Biology*, edited by J. A. Freund and T. Pöschel, Lecture Notes in Physics Vol. 557 (Springer, Berlin, 2000), p. 353.
[31] S. Saikia and M. C. Mahato, Physica A **389**, 4052 (2010), and references therein.
[32] K. Sekimoto, J. Phys. Soc. Jpn. **66**, 1234 (1997).
[33] M. I. Dykman, R. Mannella, P. V. E. McClintock, and N. G. Stocks, Phys. Rev. Lett. **65**, 48 (1990).